Non-Linear Dependence of Deflection Angle on Beam Steering Control Grid Displacement in Accelerator for N-NBI*)

Junichi HIRATSUKA, Masaya HANADA, Naotaka UMEDA, Atsushi KOJIMA, Mieko KASHIWAGI, Kazuhiro WATANABE, Hiroyuki TOBARI and Masafumi YOSHIDA

Japan Atomic Energy Agency (JAEA), 801-1 Mukoyama, Naka-shi, Ibaraki 311-0193, Japan

(Received 25 November 2014 / Accepted 18 March 2015)

To produce high current density (> 200 A/m^2), high-energy (> 1 MeV) negative ion beams for long pulse duration time (1 hour) for International Thermo-nuclear Experimental Reactor (ITER), the suppression of the direct interception of the negative ions with the grids has been carefully investigated with studying the deflection angle by aperture displacement technique. The non-linear dependence of the deflection angle appears at the aperture diameter of > 14 mm on a steering control grid (SCG). From this dependence, the aperture diameter and the offset distance of the SCG has been designed to be 16 mm and 0.7 mm, respectively and tested in a prototype accelerator for ITER. Each of the beamlets on the multiple apertures is properly steered with compensation of the deflection due to the residual magnetic field in the accelerator and the grid power loading was significantly reduced. It resulted in a 10% enhancement of the accelerated beam current.

Keywords: ITER, neutral beam injection, accelerator, negative ion, beam steering control, electrostatic lens, space charge, MeV accelerator

DOI: 10.1585/pfr.10.3405045

1. Introduction

A high power neutral beam injector based on a high energy negative ion source (N-NBI) is a promising candidate device of heating and current drive for future fusion reactors. In ITER, beam sources are designed to produce 200 A/m^2, 1 MeV negative ion beam for 1 hour [1]. In order to realize such high power and long pulse negative ion beams, proof-of-principle experiment has been performed with a prototype accelerator for ITER in Japan Atomic Energy Agency, called as MeV accelerator [2–4].

One of the critical issues for the high power and long pulse negative ion beams is the grid power loading of the accelerator.

The observation after the previous experiment shows that there were impact scars by ions around the apertures on the steering control grid (SCG) [5]. From this observation and the measurement of the grid current, secondary electrons was suggested to be generated from SCG and then accelerated with negative ions. Some of the secondary electrons were deflected by residual magnetic field and impinged on the acceleration grids. Therefore, interception of the ions with SCG should be suppressed.

The SCG is generally used to compensate the beam deflection due to the residual magnetic field created by the permanent magnets embedded in an extraction grid (EXG) and the filter magnetic field in the negative ion source. The center of the aperture of the SCG was displaced to be 0.5 mm with respect to the EXG that is placed at upstream of the SCG. The design of the displacement was based on the thin lens theory [6, 7].

The impact scars on the SCG shows the interception of the negative ion beams, which suggests the aperture diameter (14 mm for the original SCG) is not sufficient for the beam diameter. However, too large aperture diameter distorts the electric field for the compensation, which results in non-linear phenomena of deflection angles. To clarify the effect of the aperture diameter on the deflection angle, careful analyses have been done for different diameters of the SCG. Then, the displacement distance and aperture diameter of SCG were optimized to minimize the direct interception of the negative ion beams with SCG with keeping a proper deflection angle. New SCG was designed based on the analysis. The designed SCG was equipped in MeV accelerator and the performance was evaluated.

2. Dependence of Deflection Angle on Aperture Diameter

In order to clarify the beam control capability of the SCG displacement with large aperture, emittance diagrams and divergence angles with several aperture diameters were calculated with a 3D beam trajectory code, OPERA-3d [8, 9]. The effects of applied voltage on grids, magnetic field by the filter magnet and space charge of negative ion beam are taken into account in the calculation. Figure 1 (a) shows the magnetic field by the filter magnet. EX represents the extractor, which is composed of plasma grid (PG), extraction grid (EXG) and beam steering con-

author's e-mail: hiratsuka.junichi@jaea.go.jp

*) This article is based on the presentation at the 24th International Toki Conference (ITC24).

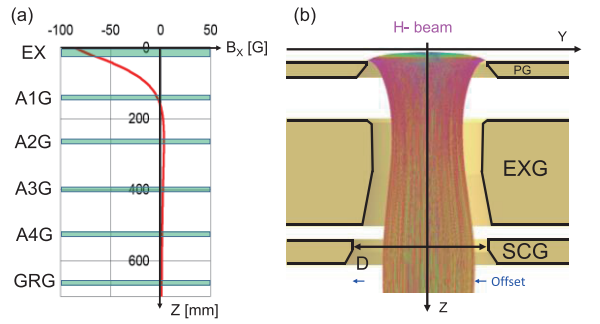

Fig. 1 (a) Magnetic field in accelerator by the filter magnet. EX denotes the extractor. (b) Trajectory of a negative ion beam (H^-) at the extractor. D denotes the aperture diameter of SCG.

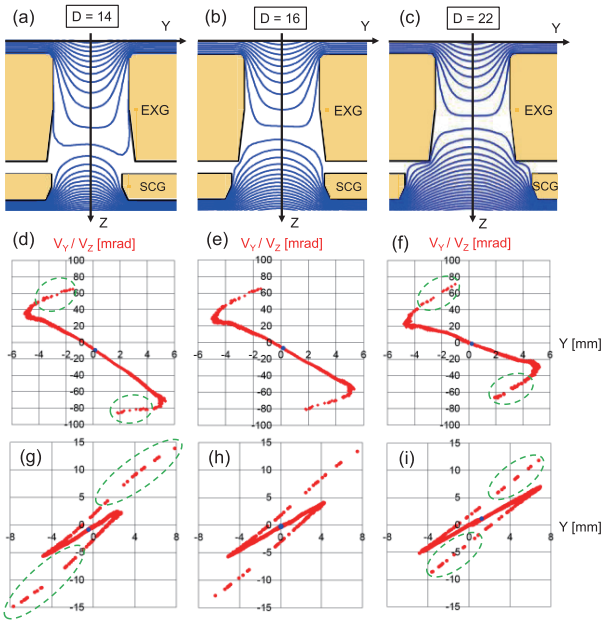

Fig. 2 Equipotential lines in the extractor (a-c). Emittance diagram of ion beam at SCG (d-f) and GRG (g-i) with three different aperture diameters of SCG (D = 14, 16, 22 mm).

trol grid (SCG). A five-stage accelerator with acceleration voltage of 1 MV, extraction voltage of 6 kV and negative hydrogen ion beam current density of 200 A/m^2 was simulated. A1G-GRG represent the acceleration grids. A calculated beam trajectory is shown in Fig. 1 (b).

Figures 2 (a-c) show cross-sectional views of the extractor with equipotential lines for three different aperture diameters. The profile of electric field is determined by the balance of voltages applied on the extraction grid and the acceleration grid, and the structure of the extractor. In a case of D = 14 mm, the electric field formed by the SCG is not disturbed due to less penetration of the field to the EXG, where the design based on the thin lens theory is available.

However, the electric field formed by acceleration gap can penetrates deeply into the EXG region with large aperture of the SCG shown in Figs. 2 (b,c). In such cases, the potential profile near the center axis of the EXG becomes flat because the extraction and acceleration fields are balanced in this region. These features are clearly observed in the case of D = 22 mm and a little in the case of D = 16 mm. In this situation, the thin lens theory is no longer applicable to the design of the SCG. This flat potential profile formed in the EXG might degrade the beam control capability of the SCG.

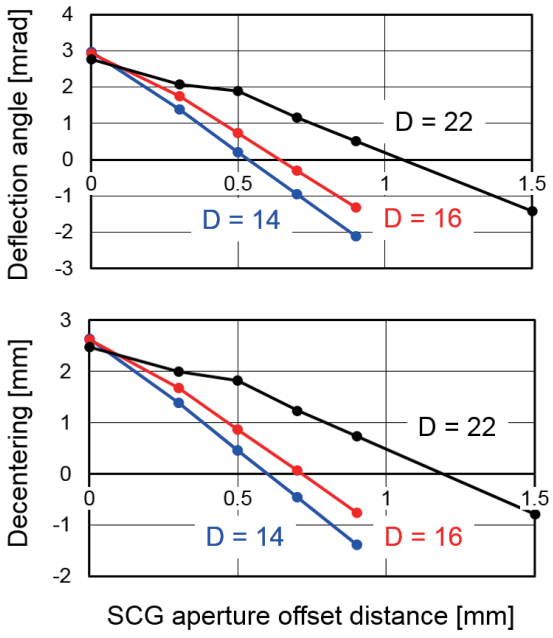

Fig. 3 Dependence of deflection at GRG on SCG aperture offset distance.

Figures 2 (d-f) and Figs. 2 (g-i) show emittance diagram of the beam at SCG and GRG, respectively. The center of the beam is marked with a blue dot in the diagrams. In this simulation, the beam deflection due to the magnetic field is observed as the positive shift of the diagram along the X and Y axes.

The dependence of beam deflection on the SCG displacement is summarized in Fig. 3. Deflection angle is defined as V_Y/V_Z of the beam center at GRG. Decentering is defined as distance between the beam center and the aperture center at GRG.

In a case of the small aperture on the SCG, the deflection angle is linearly controlled by the aperture displacement. However, large aperture of D = 22 mm has nonlinear response to the aperture displacement. This nonlinear response to the displacement is caused by the flatness of equipotential lines, which appears at the aperture diameter of > 14 mm.

Other important parameters to design the SCG is the divergence angle. Due to the weak electric field with large aperture, beam convergence capability was also degraded. Because the convergence of beam is caused by the electric field along Y-axis in Figs. 2 (a-c), the beam is expanded

with extraction electric field at PG-EXG and converged with acceleration electric field at EXG-SCG.

In Fig. 2 (g), the beam core is converged by the acceleration electric field at SCG. However, expanded particles (green-circled) were observed due to over-focusing by strong electric field at the edge of SCG. In the case of the large aperture on SCG as shown in Fig. 2 (i), because the equipotential line is flat in the EXG and acceleration electric field is weak, low focusing capability was seen from the small divergence angle of green-circled particles and large for the beam core.

Because the green-circled particles with high-divergence angle cause the heat load in the accelerator, the number of such particles should be reduced. Therefore, the effective divergence angle was investigated in terms of the aperture diameter of the SCG as shown in Fig. 4. Here, the effective divergence angle θ is defined as

$$\theta = \sqrt{\frac{\sum |Y - Y_0|\, j\, (V_Y/V_Z)^2}{\sum |Y - Y_0|\, j}}, \quad (1)$$

where Y_0 and j denote position of the beam center and current density of particle, respectively. The summation is operated for all particles. For $D < 16$ mm, divergence angle is larger with smaller aperture because of the large number of the broader expanding particles (green circled in Fig. 2). For $D > 16$ mm, divergence angle is larger with larger aperture of SCG because divergence of beam core is large due to weak electric field at SCG. Therefore, 16 mm of SCG aperture diameter is optimum for divergence angle. Transmission ratio at $D = 16$ mm is 1.0, which means no direct interception on SCG. Dependence of deflection angle and decentering at GRG on aperture diameter are also plotted in Fig. 4. These increase drastically with decreasing beam transmission at SCG for $D < 13$ mm. This is because beam extracted from the center of aperture is deflected toward the side of lower density by the effect of space charge when a part of the beam is scraped away by impingement on SCG.

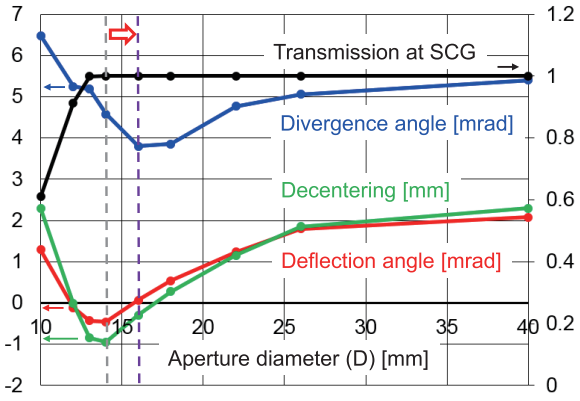

Fig. 4 Divergence angle (blue), deflection angle (red), decentering (green) after GRG vs. SCG aperture diameter. Transmission ratio at SCG is also plotted. Dashed lines denote the aperture diameter of original (grey) and new (purple) SCG.

Note that transmission ratio at SCG is 1.0 even with the original SCG ($D = 14$ mm). It suggests the impact scars on SCG may be caused by the direct interception of beam halo [10]. The trajectory of beam halo was not calculated in the simulation because model of beam halo production is inadequate. Even though there is no interception, the simulation is still useful to predict heat load on grids because beam halo is at the edge of the beam. In fact, clearance between beam and a grid in the simulation has strong correlation with heat load on the grid in experiment. Heat load is higher when the clearance is smaller.

Extractor with new SCG was designed based on the analysis. Enlargement of SCG leads to non-linear dependence of deflection angle and beam expansion due to the non-linear feature. In order to keep small beam divergence, aperture diameter of SCG is determined to be 16 mm. Dependence of deflection angle is non-linear at the diameter. In order to keep a proper deflection, aperture displacement of SCG is determined to be 0.7 mm. Following shows experimental results to evaluate beam transmission improvement and beam steering ability for new extractor.

3. Experimental Results

Beam acceleration experiment was performed to confirm the performance of the designed extractor with new SCG on the basis of the analysis above. A five-stage MAMuG accelerator, MeV accelerator, was used to produce high energy hydrogen negative ion beam. Acceleration voltage $V_{acc} = 800$ kV, extraction voltage $V_{ext} = 4.2$ - 4.3 kV and pressure in the ion source $P_s = 0.3$ Pa. Arc power for arc discharge in the ion source P_{arc} was scanned to examine achievable beam current.

Figure 5 shows the accelerated beam current measured on the beam dump and total heat load on the acceleration grids with the original ($D = 14$ mm) and new ($D = 16$ mm) extractor. Maximum beam current increased 10% with the new extractor, which reveals the beam current was limited by direct interception of beam on the extractor and the beam transmission was improved by enlarging aperture diameter of SCG.

The total heat load on the grids decreased. The heat load on the extractor and the acceleration grids measured at the arc power $P_{arc} = 17$ kW (green line in Figs. 5 (a,b)) is shown in Fig. 6. The heat load on the extractor decreased by 41%, which is caused by reduction of direct interception of negative ion beams on SCG by enlarging aperture diameter of SCG.

Further, the heat loads on the upstream grids decreased. In particular, the heat load on the first acceleration grid decreased by 46% from the value before modifying SCG. The drastic change is caused by suppression of secondary electron emission from SCG, which is resulted from the reduction of direct interception on SCG. In fact,

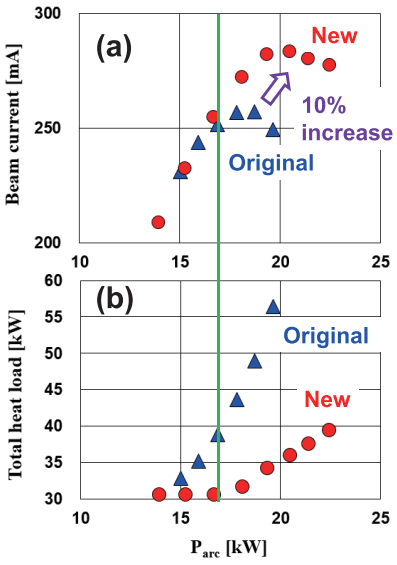

Fig. 5 (a) Accelerated beam current measured on the beam dump. (b) Total heat load on the acceleration grids.

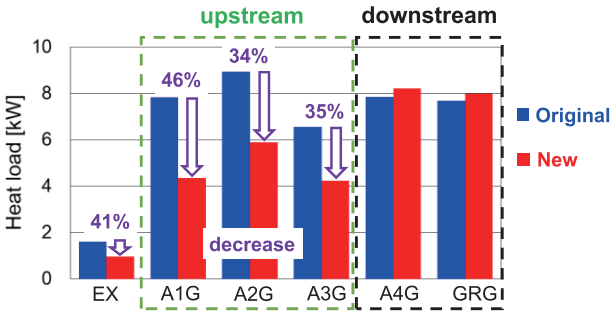

Fig. 6 Heat load on the extractor (EX) and the acceleration grids.

the total current into acceleration grids (A1G-A4G) and ground potential (GRG, beam dump and wall of beamline) decreased from 365 mA to 333 mA. It means reduction of current enhancement by secondary electron emission from SCG.

Changes of the heat load on the downstream grids (A4G and GRG) were quite small. It indicates that beam decentering is small enough because the beam steering control worked well. The slight increase of heat load (4.5% and 3.5%, respectively) may be caused by negative ions which was intercepted by SCG before enlarging the aperture diameter.

4. Summary

Beam control capability of the SCG displacement with large SCG aperture was investigated. Non-linear response to the SCG aperture displacement was observed at the diameter of > 14 mm. The non-linearity is caused by a flat potential profile near the center axis of the EXG. The flat potential profile also change beam convergence capability. Low focusing capability was observed with large aperture of the SCG due to a weak focusing electric field. With small SCG aperture, expanded beamlets were observed due to over-focusing by strong electric field at the edge of the SCG. 16 mm of SCG aperture diameter is optimum for divergence angle.

New extractor for negative ion accelerator for ITER NBI was designed based on the analysis to have 16 mm diameter and 0.7 mm of the aperture offset distance. The new extractor was equipped in the MeV accelerator. The acceleration beam current increased by a factor of 1.1, which leads to a drastic reduction of the power loading on upstream acceleration grids. The reduction is caused by suppression of secondary electron emission from SCG. The improvement of the performance of extractor contributes to the design of extractor for ITER.

[1] R. Hemsworth *et al.*, Nucl. Fusion **49**, 045006 (2009).
[2] T. Inoue *et al.*, Nucl. Fusion **46**, S379 (2006).
[3] M. Taniguchi *et al.*, Rev. Sci. Instrum. **77**, 03A514 (2006).
[4] N. Umeda *et al.*, Rev. Sci. Instrum. **85**, 02B304 (2014).
[5] N. Umeda *et al.*, "Long pulse acceleration of MeV class high power density negative H- ion beam for ITER", to be published in AIP Conf. Proc. NIBS 2014.
[6] T. Inoue *et al.*, JAERI-Tech 2000-023 (2000).
[7] M. Kashiwagi *et al.*, Rev. Sci. Instrum. **83**, 02B119 (2012).
[8] M. Kashiwagi *et al.*, Rev. Sci. Instrum. **81**, 02B113 (2010).
[9] Cobham Ltd. OPERA-3d Design software, http://www.cobham.com/
[10] H.P.L. de Esch and L. Svensson, Fusion Eng. Des. **86**, 363 (2011).